LA-UR-02-2251
Approved for public release; distribution is unlimited.

Title: **Uncertainty Quantification of a Containment Vessel Dynamic Response Subjected to High-Explosive Detonation Impulse Loading**

Author(s): Edward A. Rodriguez, Jason E. Pepin, Ben H. Thacker and David S. Riha

Submitted to: 43rd AIAA/ASME/ASCE/AHS/ASC: Structures, Structural Dynamics, and Materials Conference and Exhibit Non-Deterministic Approaches Forum, April 22-25, 2002, Denver, CO

http://lib-www.lanl.gov/cgi-bin/getfile?00818817.pdf

AIAA 2002-1567

Uncertainty Quantification of a Containment Vessel Dynamic Response Subjected to High-Explosive Detonation Impulse Loading

E. A. Rodriguez, J. E. Pepin,
Los Alamos National Laboratory
Los Alamos, NM

B. H. Thacker, D. S. Riha,
Southwest Research Institute
San Antonio, TX

43rd AIAA/ASME/ASCE/AHS/ASC
Structures, Structural Dynamics, and Materials
Conference and Exhibit
Non-Deterministic Approaches Forum
April 22-25, 2002
Denver, CO

UNCERTAINTY QUANTIFICATION OF A CONTAINMENT VESSEL DYNAMIC RESPONSE SUBJECTED TO HIGH-EXPLOSIVE DETONATION IMPULSE LOADING

Edward A. Rodriguez[(1)], Jason E. Pepin[(1)], Ben H. Thacker[(2)] and David S. Riha[(3)]

Technical Staff Member[(1)]
Engineering Sciences & Applications Division
Los Alamos National Laboratory
MS P946
Los Alamos, NM 87545

Manager[(2)]/Senior Research Engineer[(3)]
Reliability and Engineering Mechanics
Southwest Research Institute
6220 Culebra Rd.
San Antonio, TX 78238

ABSTRACT

Los Alamos National Laboratory (LANL), in cooperation with Southwest Research Institute, has been developing capabilities to provide reliability-based structural evaluation techniques for performing weapon component and system reliability assessments. The development and applications of Probabilistic Structural Analysis Methods (PSAM) is an important ingredient in the overall weapon reliability assessments. Focus, herein, is placed on the uncertainty quantification associated with the structural response of a containment vessel for high-explosive (HE) experiments. The probabilistic dynamic response of the vessel is evaluated through the coupling of the probabilistic code NESSUS[1] with the non-linear structural dynamics code, DYNA-3D[2]. The probabilistic model includes variations in geometry and mechanical properties, such as Young's Modulus, yield strength, and material flow characteristics. Finally, the probability of exceeding a specified strain limit, which is related to vessel failure, is determined.

INTRODUCTION

Over the past 30 years, Los Alamos National Laboratory (LANL), under the auspices of the U.S. Department of Energy, has been conducting confined high explosion experiments utilizing large, spherical, steel pressure vessels. Design of these spherical vessels was originally accomplished by maintaining that the vessel's kinetic energy, developed from the detonation impulse loading, be equilibrated by the elastic strain energy inherent in the vessel. Within the last decade, designs have been accomplished utilizing sophisticated and advanced 3D computer codes that address both the detonation hydrodynamics and the vessel's highly nonlinear structural response.

Cylindrical and spherical pressure vessels are used to contain the effects of high explosions. In some cases, the vessel is designed for one-time use only, efficiently utilizing the significant plastic energy absorption capability of ductile vessel materials[3]. Alternatively, the vessel can be designed for multiple use, in which case the material response is restricted to the elastic range[4].

Understanding of the dynamic events under detonation conditions is the first step towards the development of a rational pressure vessel design criteria. The multiple-use pressure vessels must, in effect, be designed with similar rules as those in Section III or VIII of the ASME Boiler & Pressure Vessel Code, hereafter referred to as the ASME Code. That is, it becomes imperative to the designer to maintain a purely elastic membrane response of the structural system. On the other hand, Environment, Safety, and Health (ESH) issues, such as waste-stream isolation, and clean-up costs associated with HE detonations within vessels, may be prohibitively expensive because of hazardous materials that may be present. In this scenario, the pressure vessel design is driven to a "single-use" mode, dictating that a more cost-effective design must be developed. The designer must start with a rational ductile failure design criterion that utilizes the plastic reserve capacity in providing structural margin. As such, quantifying uncertainties associated with loading functions, geometry (i.e., radius and thickness), fabrication, and material properties is of paramount importance when the design of these containment vessels is within the plastic regime.

The containment vessel illustrated is a 6-ft inside diameter, manufactured from HSLA-100 steel, spherical vessel. Results are presented herein for a particular explosive test, with probability density functions describing the vessel radius and thickness, and material parameters. No attempt is made, in this paper, to describe the loading function on a probabilistic basis. This will be accomplished in an upcoming study describing the variation of HE mass resulting in pressure-time history PDF.

The containment vessel is shown in Fig. 1, and consists of a minimum 2.0-in wall thickness HSLA-100 spherical shell with three ports. It is subjected to the transient pressure loading for a quantity of HE, up to a maximum charge size of 40 lbs. equivalent TNT.

Figure 1: LANL 6-ft. ID containment vessel.

1. DESCRIPTION OF CONTAINMENT VESSEL

The containment vessel is a spherical vessel with three access ports: two 16-inch ports aligned in one axis on the sides of the vessel and a single 22-inch port at the top "north pole" of the vessel. The vessel has an inside diameter of 72 inches and a 2 inch nominal wall thickness. The vessel is fabricated from HSLA-100 steel, chosen for its high strength, high fracture toughness, and no requirement for post weld heat treatment.

The vessel's three ports must maintain a seal during use to prevent any release of reaction product gases or material to the external environment. Each door is connected to the vessel with 64 high strength bolts, and four separate seals at each door ensure a positive pressure seal.

2. DETERMINSTIC ANALYSIS

A series of hydrodynamic and structural analyses of the spherical containment vessel were performed using a combination of two numerical techniques. Using an uncoupled approach, the transient pressures acting on the inner surface of the vessel were computed using the Eulerian hydrodynamics code, CTH, which simulated the HE burn, the internal gas dynamics, and shock wave propagation. The HE was modeled as spherically symmetric with the initiating burn taking place at the center of the sphere. The vessel's structural response to these pressures was then analyzed[5] using the DYNA-3D explicit finite element structural dynamics code. In this section, we summarize the results of the structural analysis of the confinement vessel subjected to a 40 lb. HE charge detonation of PBX-9501 ignited at the center of the vessel.

The simulation required the use of a large, detailed mesh to accurately represent the dynamic response of the vessel and to adequately resolve the stresses and discontinuities caused by various engineering features such as the bolts connecting the doors to their nozzles. Taking advantage of two planes of symmetry, one quarter of the structure was meshed using approximately one million hex elements. Six hex elements were used through the 2-inch wall thickness to accurately simulate the bending behavior of the vessel wall. The one-quarter symmetry model is shown in Figure 2. The structural response simulation used an explicit finite element code called PARADYN, which is a massively parallel version of DYNA-3D, a nonlinear, explicit Lagrangian finite element analysis code for three-dimensional transient structural mechanics. PARADYN was run on 504 processors of Los Alamos National Laboratory's Accelerated Strategic Computing Initiative platform "Blue Mountain," which is an interconnected array of independent SGI (Silicon Graphics, Inc.) computers. The containment vessel can be handled on Blue Mountain computer with approximately 2.5 hours of run time. The same analysis would have taken about 35 days when run on a single processor.

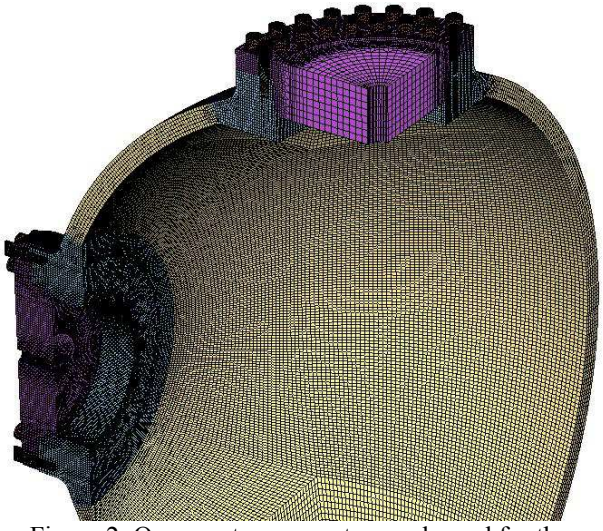

Figure 2: One quarter symmetry mesh used for the structural analysis.

The pressure-time history used for the 40 lb HE load case, as shown in Figure 3, was calculated for a duration of approximately 7 ms, which is more than

sufficient to cover the initial blast loading and several subsequent reverberations inside of the vessel. Confirmatory analyses have shown[6,7] that a smaller duration (~ 2-ms) is adequate to represent the initial impulse loading providing the driving energy to the vessel. After the 7 ms of computed pressure loading, the pressure inside the vessel was taken as constant, that being the residual quasi-static pressure resulting from the expansion of reaction product gases. Numerical computations for the structural analysis were carried out to 20 ms duration, a time considered far enough removed from the initial pressure spike to capture the peak dynamic response. The vessel initially deforms in a "breathing mode," an almost uniform radial expansion of the entire vessel and ports. Because of the asymmetry of the vessel's ports, in terms of mass and stiffness, the breathing mode degenerates after a couple of cycles into a more complex combination of bending/extensional modes as shown in Figure 4.

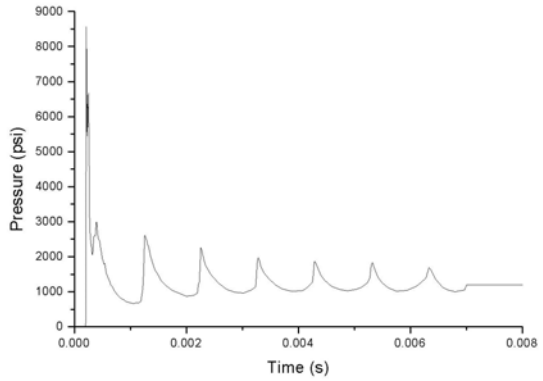

Figure 3: Pressure time history for the center detonated 40 lb HE load case.

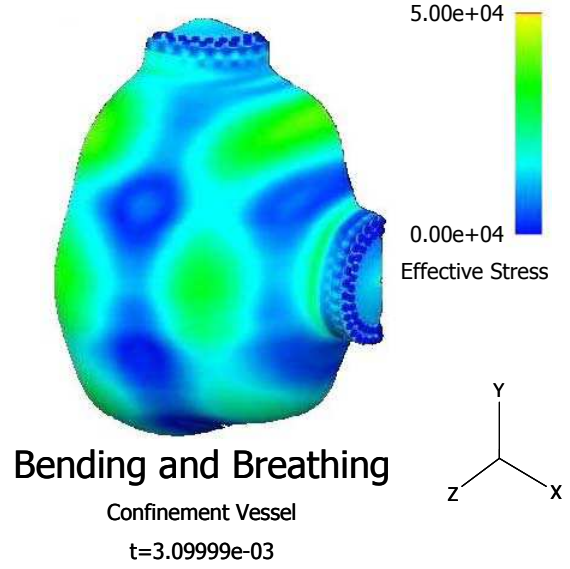

Figure 4: Structural response of the containment vessel.

Stresses caused by high-order bending modes, during the time history, are significantly greater than the stresses caused by the initial breathing response. Even well after the initial load and unload, the dynamic stress waves propagate through the vessel, and at certain times, combine to cause plastic straining in the vessel wall. Pure membrane stresses are developed only during the initial vessel response, the breathing mode. As shown in Figure 5, a unique combination of localized bending and membrane stresses causes a small amount of plastic strain to occur at the bottom of the vessel at 5 ms.

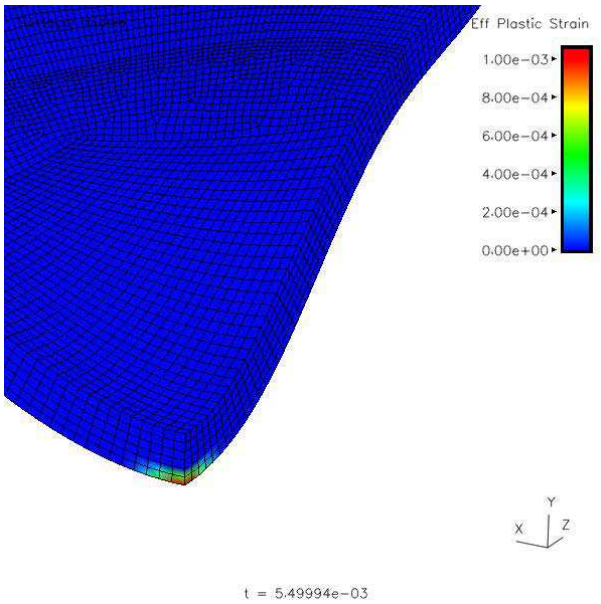

Figure 5: Plastic strain occurs at the bottom of the confinement vessel for the 40 lb HE load case.

3. PROBABILISTIC ANALYSIS

After investigation of the deterministic response of the vessel and where maximum responses occurred, the equivalent plastic strain at the bottom of the vessel was selected as the response metric. To quantify the uncertainty associated with the plastic strain occurring at the bottom of the containment vessel, a probabilistic analysis was performed with the vessel geometry and material properties as random variables.

Efficient probabilistic methods were used to calculate the probabilistic response of the containment vessel[8]. These methods have been primarily developed for complex computational systems requiring time-consuming calculations, the results of which have been shown to approach the exact solution obtained from traditional Monte Carlo methods using significantly fewer function evaluations [9].

Most Probable Point (MPP) Methods

A class of probabilistic methods based on the most probable point (MPP) are becoming routinely used as a means of reducing the number of *g*-function evaluations from that of brute-force Monte Carlo simulation. Although many variations have been proposed, the best-known and most widely-used MPP-based methods include the first-order reliability method (FORM) [9], second-order reliability method (SORM) [9], and advanced mean value (AMV) [10].

The basic steps involved in MPP-based methods are as follows: (1) Obtain an approximate fit to the exact *g*-function at X^*, where X^* is initially the mean random variable values; (2) Transform the original, non-normal random variables into independent, normal random variables u [9]; (3) Calculate the minimum distance, β (or safety index), from the origin of the joint PDF. to the limit state surface, $g = 0$. This point, u^*, on the limit state surface is the most probable point (MPP) in the u-space; (4) Approximate the *g*-function $g(u)$ at u^* using a first or second-order polynomial function; and (5) Solve the resulting problem using available analytical solutions [9].

Step (1), which involves evaluating the *g*-function, represents the main computational burden in the above steps. Once a polynomial expression for the *g*-function is established, it is a numerically simple task to compute the failure probability and associated MPP. Because of this, the complete response CDF can be computed very quickly by repeating steps (2)-(4) for different z_0 values. The resulting locus of MPP's is efficiently used in the advanced mean value algorithm (discussed next) to iteratively improve the probability estimates in the tail regions.

Advanced Mean Value (AMV) Method

The advanced mean value class of methods are most suitable for complicated but well-behaved response functions requiring computationally-intensive calculations. Assuming that the response function is smooth and a Taylor's series expansion of Z exists at the mean values, the mean value Z-function can be expressed as

$$Z_{MV} = Z(\mu) + \sum_{i=1}^{n} \frac{\partial Z}{\partial X_i}\Big|_{\mu_i} (X_i - \mu_i) + H(\mathbf{X}) \quad (1)$$

where Z_{MV} is a random variable representing the sum of the first order terms and $H(X)$ represents the higher-order terms.

For nonlinear response functions, the MV first-order solution obtained by using Equation 1 may not be sufficiently accurate. For simple problems, it is possible to use higher-order expansions to improve the accuracy. For example, a mean-value second-order solution can be obtained by retaining second-order terms in the series expansion. However, for problems involving implicit functions and large n, the higher-order approach becomes difficult and inefficient.

The AMV method improves upon the MV method by using a simple correction procedure to compensate for the errors introduced from the truncation of the Taylor's series. The AMV model is defined as

$$Z_{AMV} = Z_{MV} + H(Z_{MV}) \quad (2)$$

where $H(Z_{MV})$ is defined as the difference between the values of Z_{MV} and Z calculated at the Most Probable Point Locus (MPPL) of Z_{MV} , which is defined by connecting the MPP's for different z_0 values. The AMV method reduces the truncation error by replacing the higher-order terms $H(X)$ by a simplified function $H(Z_{MV})$. As a result of this approximation, the truncation error is not optimum; however, because the Z-function correction points are usually close to the exact MPP's, the AMV solution provides a reasonably good solution.

The AMV solution can be improved by using an improved expansion point, which can be done typically by an optimization procedure or an iteration procedure. Based initially on Z_{MV} and by keeping track of the MPPL, the exact MPP for a particular limit state $Z(X) - z_0$ can be computed to establish the AMV+ model, which is defined as

$$Z_{AMV+} = Z(\mathbf{X}^*) + \sum_{i=1}^{n} \frac{\partial Z}{\partial X_i}\Big|_{X_i^*} (X_i - \chi_i^*) + H(\mathbf{X}) \quad (3)$$

where X^* is the converged MPP. The AMV-based methods have been implemented in NESSUS and validated using numerous problems [9,10].

Probabilistic Sensitivity Analysis

For design purposes, it is important to know which problem parameters are the most important and the degree to which they control the design. This can be accomplished by performing sensitivity analyses. In a deterministic analysis where each problem variable is single-valued, design sensitivities can be computed that quantify the change in the performance measure due to

a change in the parameter value, i.e., $\partial Z/\partial X_i$. As stated earlier, each random input variable is characterized by a mean value, a standard deviation, and a distribution type. That is, three parameters are defined as opposed to just one. The performance measure is the exceedance probability (or safety index). Sensitivity measures are needed then to reflect the relative importance of each of the probabilistic parameters on the probability of exceedance. NESSUS computes probabilistic based sensitivities for both MPP and sampling based methods; details are given by Thacker [8]. The sensitivity computed as a by-product of MPP-based methods is

$$\alpha_i = \frac{\partial \beta}{\partial u_i} \tag{4}$$

measures the change in the safety index with respect to the standard normal variate *u*. Although useful for providing an importance ranking, this sensitivity is difficult to use in design because *u* is a function of the variable's mean, standard deviation, and distribution. Two other sensitivities that are more useful for design (and for importance ranking as well) include

$$S_\mu = \frac{\partial p_I}{\partial \mu_i} \frac{\sigma_i}{p_I} \tag{5}$$

which measures the change in the probability of exceedance with respect to the mean value; and

$$S_\sigma = \frac{\partial p_I}{\partial \sigma_i} \frac{\sigma_i}{p_I} \tag{6}$$

which measures the change in the probability of exceedance with respect to the standard deviation. Multiplying by σ_i and dividing by p_I non-dimensionalizes and normalizes the sensitivity to facilitate comparison between variables. The sensitivities given by Equations 5 and 6 are computed for both component and system probabilistic analysis.

The four random variables are radius of the vessel wall (radius), thickness of the vessel wall (thickness), modulus of elasticity (E), and yield stress (S_y) of the HSLA steel. A summary of the probabilistic inputs is included in Table 1. The properties for radius and thickness are based on a series of quality control inspection tests that were performed by the vessel manufacturer. The coefficients of variation for the material properties are based on engineering judgment. In this case, the material of the entire vessel, excluding the bolts, is taken to be a random variable.

Table 1: Probabilistic inputs for the containment vessel random variables

Variable	PDF	σ	μ	COV
Radius (in)	Normal	37.0	0.0521	0.00141
Thick (in)	Lognormal	2.0	0.08667	0.04333
E (lb/in^2)	Lognormal	29.0E+06	1.0E+06	0.03448
S_y (lb/in^2)	Normal	106.0E+03	4.0E+03	0.03774

When the thickness and radius random variables are perturbed, the nodal coordinates of the finite element model change with the exception of the three access ports in the vessel, which remain constant in size and move only to accommodate the changing wall dimensions. This was accomplished in NESSUS by defining a set of scale factors that defined how much and in what direction each nodal coordinate was to move for a given perturbation in both the thickness and radius. These effects are cumulative so that thickness and radius can be perturbed simultaneously. Once these scale factors are defined and input to NESSUS, the probabilistic analysis, whether simulation or AMV+, can be performed without further user intervention.

The response metric for the probabilistic analysis is the maximum equivalent plastic strain occurring over all times at the bottom of the vessel finite element model. Using NESSUS, the iterative Advanced Mean Value (AMV+) method was used to calculate a CDF for equivalent plastic strain. Also, Latin Hypercube Simulation (LHS)[11] with 100 samples was performed to verify the correctness of the AMV+ solution near the mean value. The CDF is plotted in Figure 6 on a linear probability scale and in Figure 7 on a standard normal probability scale. As shown, the LHS and AMV+ results are in excellent agreement. For far fewer finite element model evaluations, the AMV+ solution is able to predict probabilities in the extreme tail regions. If failure were to be assumed when the equivalent plastic strain exceeded some critical value, then the CDF shown in Figures 6 and 7 directly provide non-failure probabilities, i.e., probability of failure $\left(p_f\right) = 1 - CDF$.

As shown in Figure 7, the CDF approaches an asymptotic state above about u = 2. This is because beyond u = 2, the vessel wall thickness becomes so thin that the deterministic model is unable to compute a converged solution. Although not simulated here, this

condition would suggest catastrophic failure such as rupture or fracture.

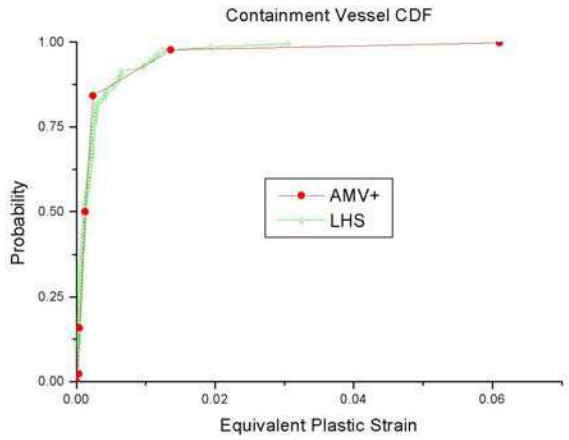

Figure 6: CDF for equivalent plastic strain at the bottom of the containment vessel.

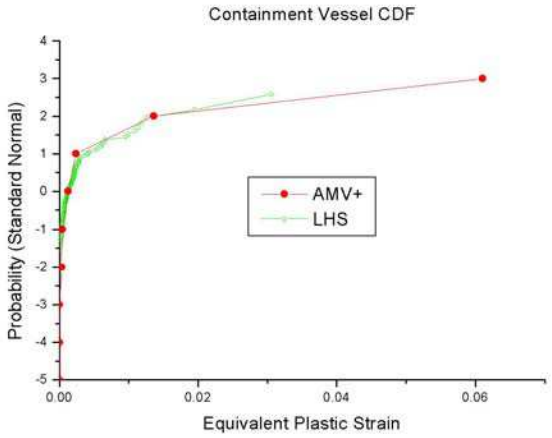

Figure 7: CDF for equivalent plastic strain plotted in standard normal space.

Probabilistic sensitivities $\left(\partial\beta/\partial\mu_i\right)\sigma_i$ and $\left(\partial\beta/\partial\sigma_i\right)\sigma_i$ are shown in Figures 8 and 9 respectively. The subscript i refers to the particular random variable and beta $\left(\beta\right)$, the safety index, is inversely proportional to p_f through the relationship $p_f = \Phi\left(-\beta\right)$ where Φ is the standard normal CDF. The sensitivities are multiplied by σ_i to nondimensionalize the values and facilitate a relative comparison between parameters. Finally, the values are normalized such that the maximum value is equal to one.

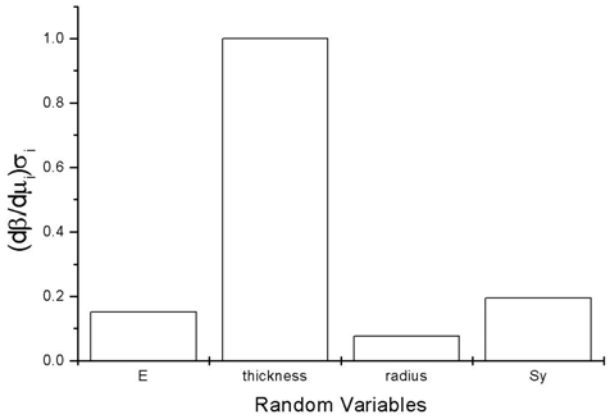

Figure 8. Probabilistic sensitivity with respect to mean (u = 3).

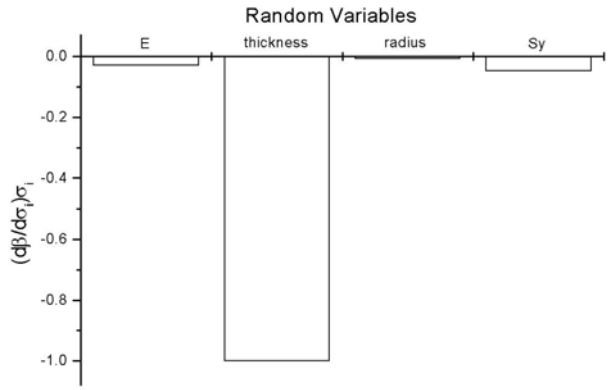

Figure 9. Probabilistic sensitivity with respect to standard deviation (u = 3).

The sensitivities shown in Figures 8 and 9 indicate how a change in the mean and standard deviation of each random variable will affect the computed probability. These results can also be used to eliminate unimportant variables from the random variables considered thus improving computational efficiency, or conversely, where resources could most effectively be focused. As shown, thickness contributes the most to the computed probability. This suggests that the most effective strategy for reducing (or at least controlling) the reliability of the vessel would be to control the thickness of the material.

4. SUMMARY

The work presented here represents an ongoing effort at Los Alamos National Laboratory to move towards increased reliance on numerical simulation and less on testing as part of the Stockpile Stewardship program. The containment vessel was selected for analysis because of the safety and mission critical nature in performing and containing small-scale dynamic experiments.

The paper demonstrates the successful application of the probabilistic analysis program NESSUS to a large ASCI scale problem (>1M elements) for the first time demonstrating its usefulness for LANL-type problems. Extensive modifications to NESSUS have been made to facilitate these calculations including the ability to link any number of numerical and/or analytical models together, support for parallel and batch job execution, and the inclusion of a graphical user interface that runs on all laboratory hardware. Future work may include additional testing to improve the characterization of the vessel thickness, coupling the hydrocode simulation of the detonation event with the structural response simulation, and incorporating alternative different failure models (fracture, burst, etc).

ACKNOWLEDGMENTS

This work was performed for the Los Alamos National Laboratory under contract No. W-7405-ENG-36 with the US Department of Energy (DOE) and the National Nuclear Security Administration (NNSA).

REFERENCES

1. **NESSUS** Users' Manual, Version 3.0, Southwest Research Institute, September 2001.

2. **DYNA-3D** User's Manual, "A Nonlinear, Explicit, Three-Dimensional Finite Element Code for Solid and Structural Mechanics," Lawrence Livermore National Laboratory, October, 1999.

3. W. E. Baker, "The Elastic-Plastic Response of Thin Spherical Shells to Internal Blast Loading," ***Journal of Applied Mechanics***, Vol. 27, pp. 139-144 (1960).

4. J. J. White and B. D. Trott, "Scaling Law for the Elastic Response of Spherical Explosion-Containment Vessels," ***Experimental Mechanics***, Vol. 20, 174-177 (1980).

5. R. Robert Stevens and Stephen P. Rojas, "Confinement Vessel Dynamic Analysis," **Los Alamos National Laboratory Report**, LA-13628-MS (1999).

6. T. A. Duffey and E. A. Rodriguez, "Ductile Failure Criteria for Design of HSLA-100 Steel Confinement Vessels," **Los Alamos National Laboratory Report**, LA-13800-MS, 2000.

7. T. A. Duffey and E. A Rodriguez, "Dynamic versus Static Pressure Loading in Confinement Vessels," **Los Alamos National Laboratory Report**, LA-13801-MS, 2000.

8. Y. T. Wu, and O. H. Burnside, "Efficient Probabilistic Structural Analysis Using an Advanced Mean value Method," **Proceedings, ASCE Specialty Conference on Probabilistic Mechanics**, 1998.

9. B. H. Thacker, et al., "Computational Methods for Structural Load and Resistance Modeling," American Institute of Aeronautics and Astronautics, **AIAA-91-0918-CP**, April 1991.

10. Y. T. Wu, et al., "Advanced Probabilistic Structural Analysis Method for Implicit Performance Functions," American Institute of Aeronautics and Astronautics, **AIAA Journal**, Vol. 2, No. 9, Sept. 1990.

11. M. D. McKay, et al., "A Comparison of Three Methods for Selecting Values of Input Variables in the Analysis of Output from a Computer Code**," Journal of Technometrics**, Vol. 21, No. 2, May 1977.